

# Severe Loss of Tritan Color Discrimination in *RPE65* Associated Leber Congenital Amaurosis

Neruban Kumaran,<sup>1,2</sup> Caterina Ripamonti,<sup>3</sup> Angelos Kalitzeos,<sup>1,2</sup> Gary S. Rubin,<sup>1,2</sup> James W. B. Bainbridge,<sup>1,2</sup> and Michel Michaelides<sup>1,2</sup>

<sup>1</sup>UCL Institute of Ophthalmology, University College London, London, United Kingdom

<sup>2</sup>Moorfields Eye Hospital, London, United Kingdom

<sup>3</sup>Cambridge Research Systems Ltd., Kent, United Kingdom

Correspondence: Michel Michaelides, UCL Institute of Ophthalmology, 11-43 Bath Street, London, EC1V 9EL, UK; michel.michaelides@ucl.ac.uk.

Submitted: August 31, 2017

Accepted: November 9, 2017

Citation: Kumaran N, Ripamonti C, Kalitzeos A, Rubin GS, Bainbridge JWB, Michaelides M. Severe Loss of tritan color discrimination in *RPE65* associated Leber congenital amaurosis. *Invest Ophthalmol Vis Sci*. 2018;59:85-93. <https://doi.org/10.1167/iovs.17-22905>

**PURPOSE.** *RPE65*-associated Leber congenital amaurosis (*RPE65*-LCA) is a progressive severe retinal dystrophy with early profound dysfunction of rod photoreceptors followed by progressive cone photoreceptor degeneration. We aim to provide detailed information about how cone dysfunction affects color discrimination.

**METHODS.** Seven adults (aged 16-21) with *RPE65*-LCA underwent monocular color discrimination assessment using the Trivector and Ellipse versions of three computerized tests: Cambridge Colour Test (CCT), low vision version of the Cambridge Colour Test (lvvCCT), and the Universal Colour Discrimination Test (UCDT). For comparison, subjects were also tested using the American Optical Hardy Rand Rittler (AO-HRR) plates. Each assessment was repeated three times.

**RESULTS.** The Trivector version of the tests demonstrated that color discrimination along the tritan axis was undetectable in four subjects, and severely reduced in three subjects. These findings were confirmed by the Ellipse version of the tests. Color discrimination along the protan and deutan axes was evident but reduced in six of seven subjects. Four of seven subjects were unable to read any of the HRR plates.

**CONCLUSIONS.** The computerized color vision tests adopted in this study provide detailed information about color discrimination in adult *RPE65*-LCA patients. The condition is associated with severe impairment of color discrimination, particularly along the tritan axis indicating possible early involvement of S-cones, with additional protan and deutan loss to a lesser extent. This psychophysical assessment strategy is likely to be valuable in measuring the impact of therapeutic intervention on cone function.

**Keywords:** color vision, retina, Leber congenital amaurosis, LCA, LCA2, clinical trials, endpoints

Leber congenital amaurosis (LCA) is thought to affect between 1 in 33,000 to 1 in 81,000,<sup>1,2</sup> and is believed to account for  $\geq 5\%$  of all inherited retinal diseases.<sup>1</sup> Presentation is from birth with severe visual impairment, nystagmus, and poor pupillary responses. While LCA is known to be progressive in nature, this can vary widely among patients. To date, 25 genes have been identified to account for approximately 70% to 80% of cases, with *RPE65*-associated LCA accounting for approximately 5% to 10%.<sup>3</sup> *RPE65* encodes a retinoid isomerase expressed in the RPE and is a critical component in the visual cycle. Following successful gene replacement in *RPE65* canine<sup>4</sup> and murine models<sup>5</sup>, human gene therapy trials have demonstrated safety and varying levels of efficacy.<sup>6-10</sup>

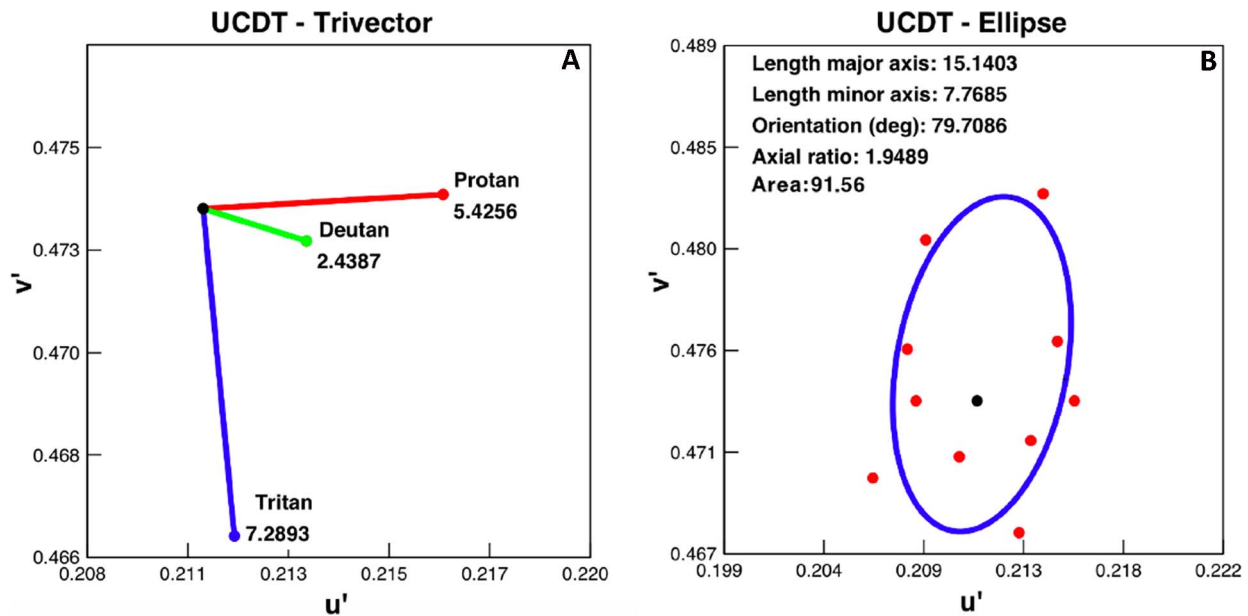
Subjects with *RPE65*-LCA have reduced or absent rod function and reduced cone-driven temporal sensitivity.<sup>11,12</sup> However, to date, little is known about how these deficiencies affect color vision in *RPE65*-LCA. Jacobson et al.<sup>13</sup> noted absence of S-cone function in all of the 6 assessed *RPE65*-LCA patients. This group further describes residual L-cone function in two other *RPE65*-LCA patients.<sup>13</sup> Lorenz et al.<sup>14</sup> also noted poorer sensitivity to blue light (mediated by S-cones) than red

light (mediated by L-cones) in *RPE65*-LCA patients. While Paunescu et al.<sup>15</sup> described residual color vision, but difficulty in blue-green discrimination, in four *RPE65*-LCA children. However, further description or quantification of color discrimination has not been made to date. This may be due in part to limitations of traditional color vision assessments, as described below.

Of the three cone classes, S-cones account for a significant minority (<10%) of the cone population. Furthermore, they are absent at the foveal center<sup>16</sup> and constitute  $5.7\% \pm 0.7\%$  of the photoreceptor mosaic imaged in vivo approximately  $1^\circ$  from fixation,<sup>17</sup> suggesting a more peripheral placement of this already infrequent cone class. Interestingly, M- and L-cones share many physiologic and genetic similarities, and considerable variability in the L:M-cone ratio has been identified in subjects with normal vision.<sup>18</sup>

Many different tests exist to assess color vision; they typically use a test stimulus of a defined chromaticity, which is compared with a reference stimulus of a different chromaticity. Pseudoisochromatic plate tests are most often used in clinical care and are based on the principles of Stilling,<sup>19</sup> where stimuli are presented on a background, with both being made





**FIGURE 1.** (A) Example of the UCDA Trivector assessment in a healthy subject. Shown next to each confusion axis are the corresponding saturation mean values. Of note, measurements have been multiplied by 10<sup>3</sup>, in keeping with previously published and accepted methods. This demonstrates good color discrimination in the protan, deutan, and tritan axes. (B) Example of the UCDA Ellipse assessment results in a healthy subject. Of note, values for major and minor axes correspond to the respective diameters of the Ellipse.

up of discrete discs that vary in size and luminance. This ensures that the object is only identifiable from its background by its chromatic difference and not from a difference in perceived luminance. Computerized color vision testing is less frequently used in clinical practice and more so in research settings. Computerized tests such as the Colour Assessment and Diagnosis test (CAD),<sup>20</sup> the Cambridge Colour Test (CCT),<sup>21</sup> the low-vision version of the Cambridge Colour Test (lvvCCT),<sup>22</sup> and the Universal Colour Discrimination Test (UCDT)<sup>23</sup> offer multiple advantages. Firstly, through using methods described below, they allow greater quantitative characterization of color discrimination. Secondly, by incorporating the “chromatophotometer,”<sup>24</sup> computerized color tests change the chromatic difference between the stimulus and the background in response to patient performance, enabling more precise measurement of color discrimination. Moreover, they are able to randomize the presentation of stimuli to counteract any learning effect.

The CCT was the first popular computerized test to measure color discrimination.<sup>21</sup> The CCT has been since shown to be suitable only for patients with a visual acuity lower, and thereby better, than 0.78 LogMAR.<sup>23</sup> Identifying the limitation of poor visual acuity in assessing color discrimination, a modified version of the CCT, the lvvCCT, was developed.<sup>22</sup> Subsequently, the UCDT was established and shown to accurately measure color discrimination in both adults and children, even with a visual acuity higher, and thereby worse, than 1.00 logMAR.<sup>23</sup>

There are two versions of each computerized test: the Trivector version and the Ellipse version. Both versions measure the amount of saturation required to discriminate a color target from a series of gray distractors. The Trivector version is a screening version because it allows rapid testing of color discrimination along three vectors; namely the protan, deutan, and tritan confusion axes. Figure 1A shows the saturation thresholds obtained from an ideal observer with normal color discrimination, with a saturation threshold of 5.43, 2.44, and 7.29 in the protan, deutan, and tritan confusion axes, respectively. The Ellipse version, shown in Figure 1B,

assesses color discrimination along more than three confusion axes, which allows an Ellipse to be determined.<sup>25</sup>

In this study, we aim to provide detailed information about how cone dysfunction in *RPE65*-LCA affects color vision by using the American Optical Hardy Rand Rittler (AO-HRR) plate test and three computerized color discrimination tests: the CCT, lvvCCT, and UCDT. The AO-HRR plate test was used for comparison, as such plate tests are commonly used in a clinical setting, while, the computerized tests were chosen as they have been shown to be effective in testing subjects with inherited or acquired color vision defects, including subjects with low vision.<sup>22,23,26–28</sup>

## METHODS

### Subjects

Seven subjects (aged 16–21) were each molecularly confirmed as having two likely disease-causing sequence variants in *RPE65* following targeted next generation sequencing of the coding regions of 176 retina-associated genes from genomic DNA extracted from peripheral blood leukocytes (performed at The Manchester Centre for Genomic Medicine, Manchester, UK). Parental blood was used to confirm the variants to be in trans by cosegregation analysis with Sanger direct sequencing, where possible. The L/M-opsin genes were not screened. The study protocol adhered to the tenets of the Declaration of Helsinki and was approved by the Moorfields Eye Hospital Ethics Committee. Informed consent was obtained from all subjects prior to entering the study.

### Assessments of Color Discrimination

All patients were assessed monocularly, with their current spectacle correction where used, using the AO-HRR chart first and then with the three computerized tests in a randomized fashion. Furthermore, the first eye tested was also randomized and all patients were instructed using standardized text instructions, specific for each individual assessment. The

TABLE 1. Neutral Points of Three Computerized Color Tests

	CCT	IvvCCT	UCDT
u'	0.1977	0.1977	0.211
v'	0.4689	0.4689	0.4735

instructions asked the patient to identify the stimulus as compared with the gray background or gray detractors (as appropriate) and provide a response using the response box. If they could not see the stimulus or a difference, subjects were asked not to respond. A demonstration test was performed binocularly for each test, to ensure that the subject had understood the instructions. For each test, the Trivector version was run first for each eye independently, followed by the Ellipse version. The Ellipse version assessed color discrimination along a subset of 10 axes equally spaced every 36°. The neutral points of each computerized test are reported in Table 1.

Each computerized test aimed to measure the minimum saturation required by the subject to discriminate the colored target from the gray background or the gray distractors. On each trial, if the observer responded correctly, the saturation of the target would decrease. Conversely, if they answered incorrectly the saturation of the target would increase. The tests used a weighted 1 up/1 down staircase<sup>29</sup> with an up/down ratio of 1/3 in order to converge on the 75% threshold. The step size used depended on the number of reversals completed. To begin with, the saturation was equal to the maximum length of the current axis that was within the color gamut of the monitor and the decreasing rate of the step size was 48% until the first reversal and 8% for the remaining reversals. The increasing rate of the step size was always 24%. The staircase consisted of six reversals and the mean of the last four reversals was taken as the threshold. More details on the adaptive method used can be found in Regan et al.<sup>21</sup>

Of note, a nonresponse was considered to be an incorrect response. If the test recorded five consecutive incorrect responses the staircase along that particular axis would terminate, with the intention to shorten testing time in those unable to discriminate a particular hue even at its maximum saturation. In this case, the staircase along that hue/axis would terminate after the first five incorrect responses instead of continuous, unnecessary, testing to achieve the required number of reversals.

The AO-HRR Plate Test score was set as the number of complete plates identified out of the 14 diagnostic plates (numbered 11–24).

Each patient underwent the above assessments of color discrimination three times on different days. The above tests took approximately 2 hours to complete (further to any breaks required by the patient), with the three sessions being performed over a range of 4 days to 11 weeks.

### Color Vision Tests

We used the AO-HRR pseudoisochromatic plates (4th edition; Richmond Products, Inc., Albuquerque, NM, USA) and the commercially available CCT, IvvCCT, and UCDT, which are included with the Metropsis system (Cambridge Research Systems Ltd., Rochester, Kent, UK). The test stimuli were presented on a calibrated 32" Display++ liquid crystal display monitor (Cambridge Research Systems Ltd., Rochester, Kent, UK) connected to an Apple iMac computer (Apple, Inc., Cupertino, CA, USA). Table 2 shows example stimuli,

advantages, and disadvantages of the four color vision assessments used in this study.

The Display++ resolution is 1920 × 1080 pixels and its frame rate is 120 Hz. It provides 16-bit RGB color resolution. A five-key RB-540 Cedrus response box (Cedrus, San Pedro, CA, USA) was used to collect observers' responses. The tests were controlled by the Metropsis system (Cambridge Research Systems Ltd., Rochester, Kent, UK).

AO-HRR plates were presented under a Daylight Illuminator (Richmond Products, Inc., Albuquerque, NM, USA) and scored using the accompanying worksheet. Best-corrected visual acuity (BCVA) was assessed using a Lighthouse (Long Island City, NY, USA) or Precision Vision Lightbox (Woodstock, IL, USA) and a stand, illuminated with 2 cool daylight 20-W fluorescent tubes (each with a color temperature of 6500 K and a color rendering index of 75).

### Stimuli

**Low-Vision Version of the Cambridge Colour Test (IvvCCT).** In this assessment, four discs are presented on a 2-cd/m<sup>2</sup> neutral background in a diamond-shaped array. Each subtends 4° at the test distance (1.5 m) and was separated by 2.5° from the adjacent discs. On each presentation, one of the discs differs in chromaticity from the remaining three (which remain of neutral hue) and the patient was asked to identify which of the four discs is different in color.<sup>22</sup>

**Cambridge Colour Test (CCT).** The CCT involves the presentation of a 5° Landolt C-like ring in four orientations, against a background that differs in chromaticity only. Based on the principles of Stilling,<sup>19</sup> the target and background are made up of many discrete discs, each with its own contour, and the luminance of the individual discs are randomized. These two maneuvers allow discrimination of the target from the background using chromaticity alone. The observer was instructed to report the position of the 1° gap in the C-like ring presented.<sup>21</sup>

**Universal Colour Discrimination Test (UCDT).** The UCDT is a two alternative forced-choice assessment involves the presentation of circles of random luminance. A subset of circles delineates a 8.58° square stimulus that varies in saturation and hue only, on the left or right hand side of the screen, with the patient being asked to distinguish the laterality.<sup>23</sup>


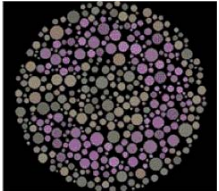
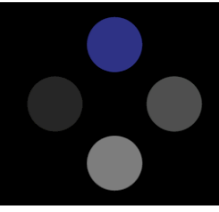
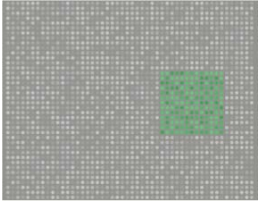
### Assessment of Best-Corrected Visual Acuity

Each patient underwent a subjective refraction and subsequent assessment of BCVA. The number of Early Treatment Diabetic Retinopathy Study (ETDRS) letters read was scored. This was performed three times, on different days, and the number of ETDRS letters read was averaged and converted into a logMAR equivalent.

### Statistical Analysis

Statistical analyses were performed using the Stata statistical software package (StataCorp, College Station, TX, USA). For Trivector assessment of the three computerized tests, a one-way repeated measures ANOVA was used to investigate any statistically significant difference in the mean saturation threshold between the three (protan, deutan, and tritan) confusion axes. In cases where a statistically significant difference was found, a post hoc pairwise comparison with Bonferroni correction was used to compare the mean saturation thresholds between the (1) protan and deutan, (2) protan and tritan, and (3) deutan and tritan axes, respectively. To minimize the clustering effect of using data from both eyes, only results from the right eye of all subjects were analyzed.

TABLE 2. Example Stimulus, Advantages, and Disadvantages of the Four Color Vision Assessments Used in This Study

Test	Example Stimulus	Advantages	Disadvantages
Hardy Rand Rittler Test		All cone classes. Quick (<5 min).	Need “good” acuity. Not sensitive to small changes. Plates can fade over time.
CCT		All cone classes. Sensitive to change. Stimuli are randomized to counteract memorization.	Need “good” acuity, due to 1° gap in C stimulus. Takes longer (~10 min).
lvvCCT		All cone classes. Sensitive to change. Stimuli are randomized to counteract memorization. Appropriate for low vision.	Takes longer (~10 min).
UCDT		All cone classes. Sensitive to change. Stimuli are randomized to counteract memorization. Appropriate for low vision. Appropriate for small visual field.	Takes longer (~10 min).

The same statistical analysis was performed on data from the left eye and provided comparable results.

tritan, and tetartan plates. A normal trichromat should be able to identify all 14 diagnostic plates.

**RESULTS**

Table 3 shows the demographics, RPE65 variants, and average BCVA for all seven subjects.

**AO-HRR Test**

Only three subjects (subjects number 4, 5, and 6) were able to read at least one full plate. The total number of plates read by these three subjects ranged from one to six. Of note, the plates read were distributed equally throughout the deutan, protan,

**Low-Vision Version of the Cambridge Colour Test (lvvCCT): Trivector Test**

Figure 2 shows the mean saturation threshold and standard error of each eye, of each patient in the protan, deutan, and tritan axes, as calculated by the Trivector assessment of the lvvCCT. As described above, a normal trichromat has a saturation threshold of less than 10 (shown by the gray shaded area in each row in Fig. 2). The maximum saturation threshold the monitor is able to present is 110 in each axis (as shown by the dotted line in each row in Fig. 2).

TABLE 3. Cohort Demographics Including Sex, Age, RPE65 Variants, and Best-Corrected Visual Acuities (logMAR)

Subject Number	Sex	Age	RPE65 Variant 1	RPE65 Nucleotide 1	RPE65 Variant 2	RPE65 Nucleotide 2	Right Eye BCVA	Left Eye BCVA
1	Female	21	c.118G>A	p.Gly40Ser	*c.955G>A	p.Glu319Lys	0.3	0.4
2	Female	20	c.989G>A	p.Cys330Tyr	*c.1443_1445delAGA	p.Glu481del	0.7	0.7
3	Male	20	c.1451G>A	p.Gly484Asp	c.1451G>A	p.Gly484Asp	0.5	0.6
4	Female	20	c.11+5G>A	Splice region	*c.1341_1342dupCT	p.Cys448SerfeTer4	0.8	0.7
5	Female	19	c.1078C>A	p.Pro363Thr	c.1078C>A	p.Pro363Thr	0.6	0.6
6	Male	18	c.370C>T	p.Arg124Ter	c.952T>A	p.Tyr318Asn	0.9	0.5
7	Male	16	c.11+5G>A	Splice region	*c.245G>A	p.Arg82Lys	0.7	0.6

\* Sequence variants preceded with an asterisk are noted to be novel.

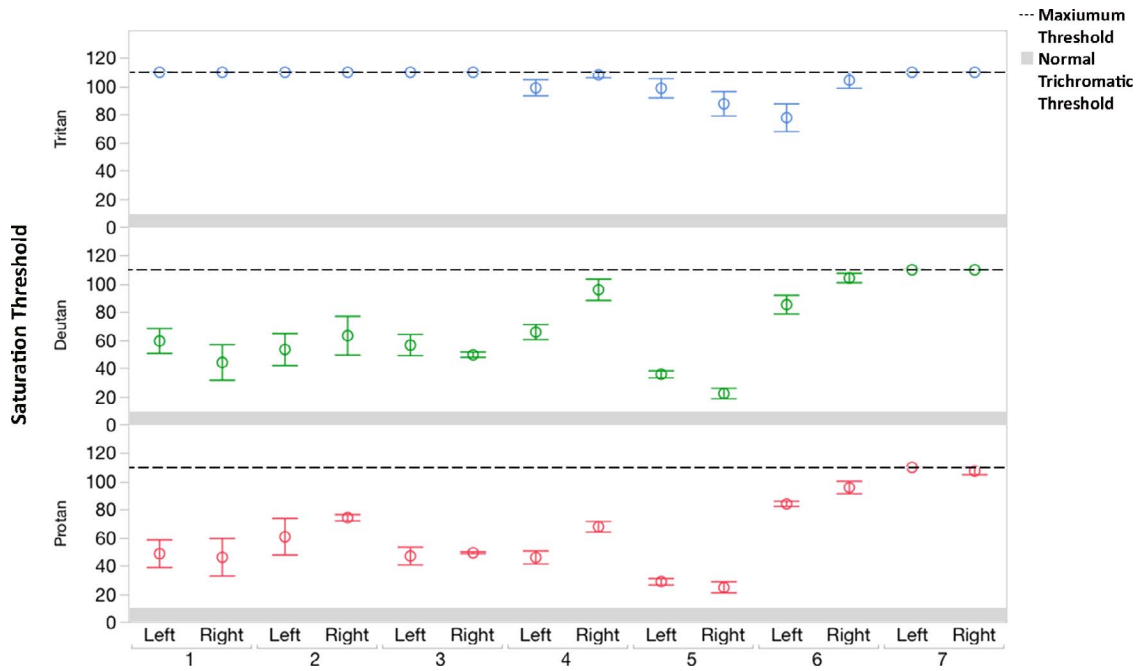


FIGURE 2. Low vision version CCT Trivector test results. Shown are the mean (symbols) and one standard error (vertical bars) of the mean saturation along the tritan (blue), deutan (green), and protan (red) axes, for each eye of each of the seven tested subjects. The dotted line in each row represents the maximum saturation threshold the monitor is able to present (110). The gray shaded area in each row corresponds to the normal trichromatic range (0-10).

Four participants (subjects 1, 2, 3, and 7) were unable to see the stimulus in the tritan axis despite presentation of a maximally saturated stimulus (Fig. 2). Conversely three participants (subjects 4, 5, and 6) were able to identify the tritan stimulus below the maximal threshold, suggesting that these participants had some color discrimination in the tritan

axis. Given that these saturation threshold values are close to the maximal level, their tritan discrimination can be described as poor. Interestingly, when reviewing the same in the protan and deutan axes, all participants, except subject 7, exhibited varying degrees of color discrimination in the protan and deutan axes.

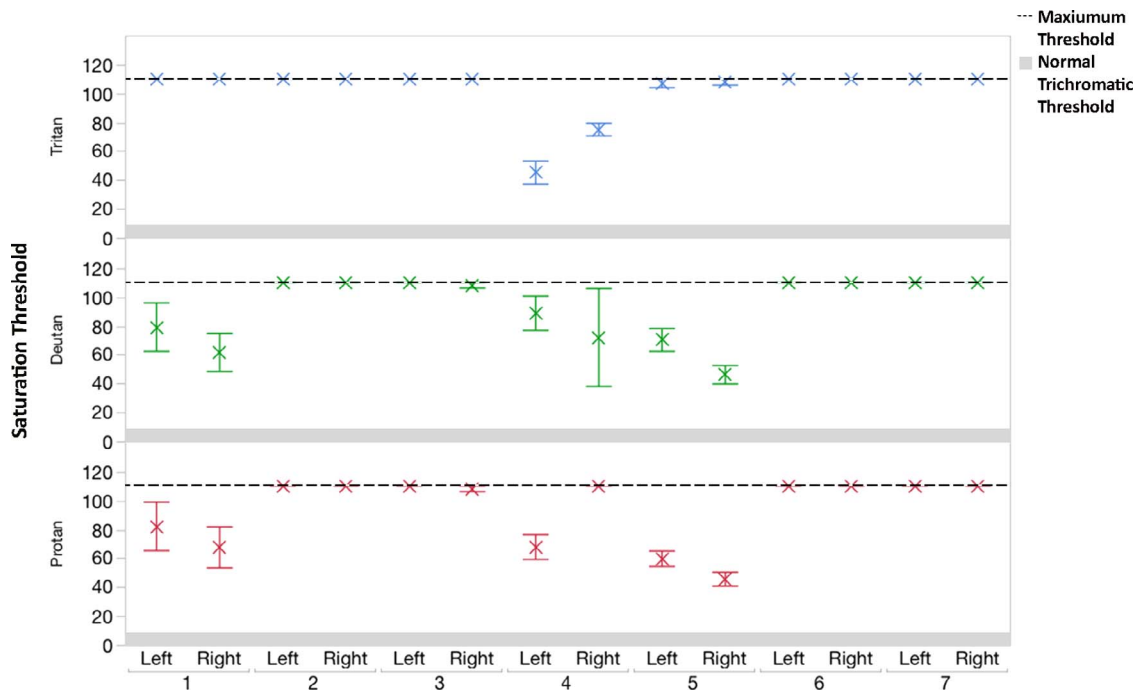


FIGURE 3. CCT Trivector test results. Shown are the mean (symbols) and one standard error (vertical bars) of the mean saturation along the tritan, deutan, and protan axes, for each eye of each of the seven tested subjects. The dotted line in each row represents the maximum saturation threshold the monitor is able to present (110). The gray shaded area in each row corresponds to the normal trichromatic range (0-10).

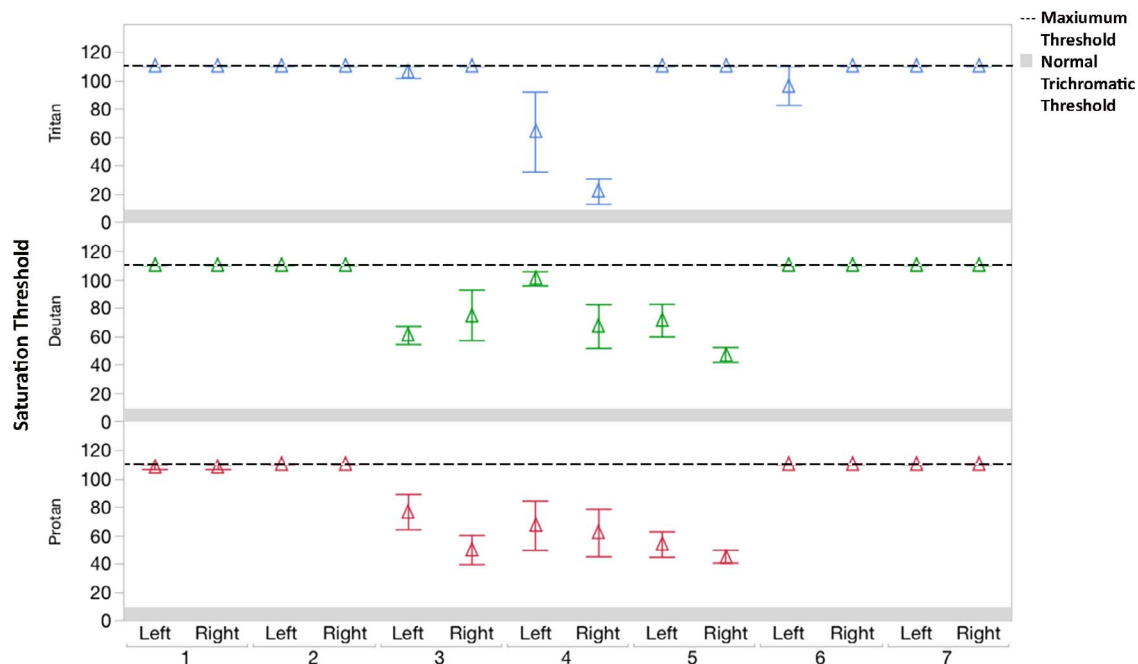


FIGURE 4. UCDT Trivector test results. Shown are the mean (symbols) and one standard error (vertical bars) of the mean saturation along the tritan, deutan, and protan axes, for each eye of each of the seven tested subjects. The dotted line in each row represents the maximum saturation threshold the monitor is able to present (110). The gray shaded area in each row represents the normal trichromatic range (0–10).

There was a statistically significant difference ( $F_{(2,12)} = 11.42$ ,  $P = 0.0017$ ) in mean saturation threshold between the three confusion axes, suggesting a difference in color discrimination between the three confusion axes. A Bonferroni post hoc test identified subjects to have a significantly better mean saturation threshold in the protan axis ( $39.44 \pm 9.15$ ,  $P = 0.003$ ) and the deutan axis ( $36.02 \pm 9.15$ ,  $P = 0.006$ ) as compared with the tritan axis. This suggests significantly worse color discrimination in the tritan axis as compared with the protan axis and the deutan axis.

### Cambridge Colour Test (CCT): Trivector Test

Figure 3 illustrates the mean saturation threshold and standard error of each eye, of each patient in the protan, deutan, and tritan axes as calculated by the Trivector assessment of the CCT. Subjects 2, 3, 6, and 7 showed no evidence of color discrimination, using the CCT trivector test, as indicated by the maximum possible saturation thresholds. Subjects 1 and 5 showed evidence of color discrimination along the deutan and protan confusion axes. Subject 4 appeared to retain color discrimination along all three confusion axes, with a markedly variable performance in the deutan axis of the right eye (as indicated by the respective error bars).

No statistically significant difference in the mean saturation threshold between the three confusion axes ( $F_{(2,12)} = 1.49$ ,  $P = 0.265$ ) was observed. This suggests that, in this cohort, while there was a trend toward worse color discrimination in the tritan axis, there was no statistically significant difference between their discrimination in the three axes, using the CCT.

### Universal Colour Discrimination Test (UCDT): Trivector Test

Figure 4 shows the mean saturation threshold and standard error of each eye, of each patient in the protan, deutan, and tritan axes as calculated by the Trivector assessment of the UCDT.

Subject 4 exhibited discrimination in all three confusion axes in both eyes, but as shown by the error bars (Fig. 4), this patient's responses were very variable in four of the six axes tested over the two eyes. Of the remaining six subjects, only subject six demonstrated residual tritan discrimination (left eye), which was both variable and at a level close to the maximum threshold the monitor is able to present. Furthermore, of these six subjects, two (subjects 3 and 5) demonstrated discrimination in the protan and deutan axes.

In keeping with the CCT Trivector results, statistical analysis did not show a statistically significant difference in the mean saturation threshold between the three axes ( $F_{(2,12)} = 0.63$ ,  $P = 0.551$ ).

### CCT, LvvCCT, and UCDT Ellipse Test

The subset of 10 saturation thresholds identified using the Ellipse test were fitted with a 'best-fit' Ellipse using a least-square procedure.<sup>30</sup> This allows color discrimination to be described using three parameters; the orientation of the Ellipse, the axial ratio (the ratio between the major and minor axes), and the area within the Ellipse. Each parameter allows quantification of a different aspect of color discrimination. The orientation of the Ellipse provides information regarding the axes in which the patient lacks discrimination and can suggest loss of tritan, protan, or deutan discrimination if it correlates with these confusion axes: the greater the axial ratio, the more selective the loss of color discrimination in the relevant confusion axis. The area within the Ellipse can provide a quantification of the discrimination ability of the patient: the smaller the area the better the color discrimination ability. Color discrimination Ellipses of a normal trichromat have an axial ratio and area within the Ellipse typically less than 2 and 340 (using a  $10^3$  unit multiplication in keeping with previously published and accepted methods), respectively.<sup>31</sup>

Figure 5 shows the mean and standard error of the areas of the best-fit color discrimination Ellipse for each test. Furthermore, the dashed line represents the maximum threshold the

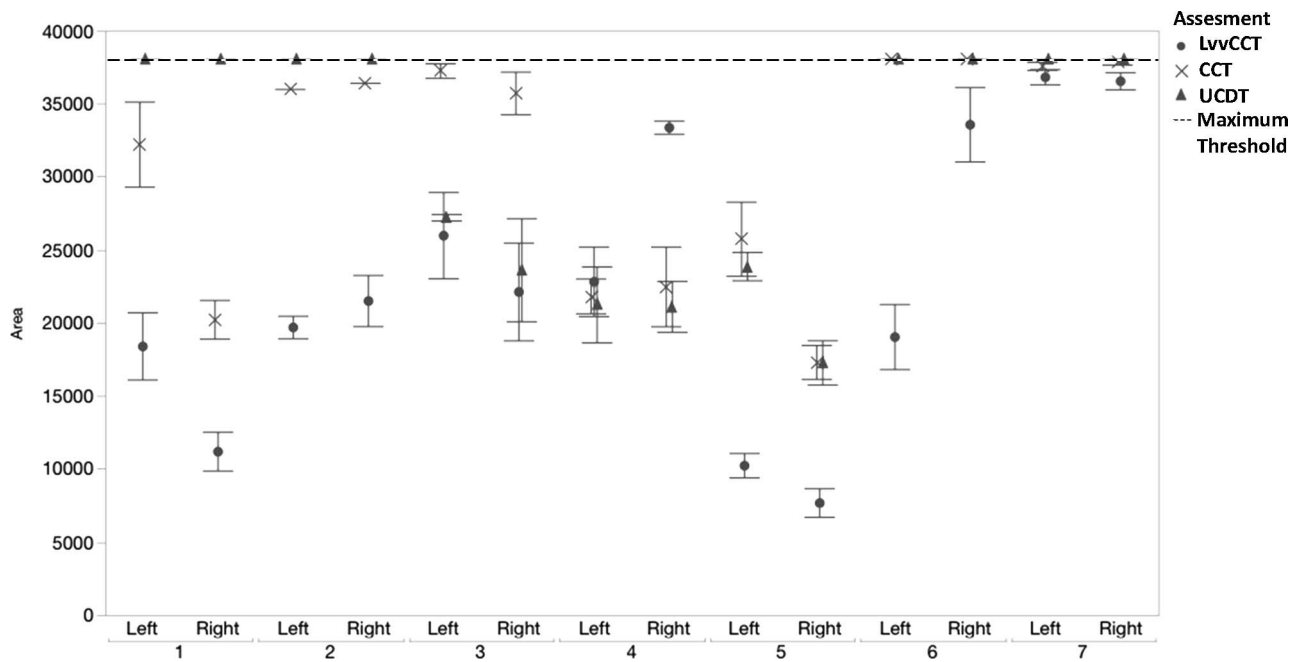


FIGURE 5. Color discrimination Ellipse areas. Shown are the mean (symbols) and one standard error (vertical bars) of the area of the Ellipse for the lvvcCT, CCT, and UCDT, for each eye of each of the seven tested subjects. The dotted line represents the maximum saturation threshold the monitor is able to present. A normal trichromatic region is from 0 to 340.

monitor is able to present. Figure 5 confirms that color discrimination can be measured, with differing variability in six of seven patients; however, subject 7 demonstrated very poor color discrimination with all three tests. The LvvcCT had a

lower average Ellipse area in five of the remaining six tested subjects than the other two tests, suggesting that these patients had better color discrimination when assessed with the lvvcCT, as compared with either the CCT or UCDT; the

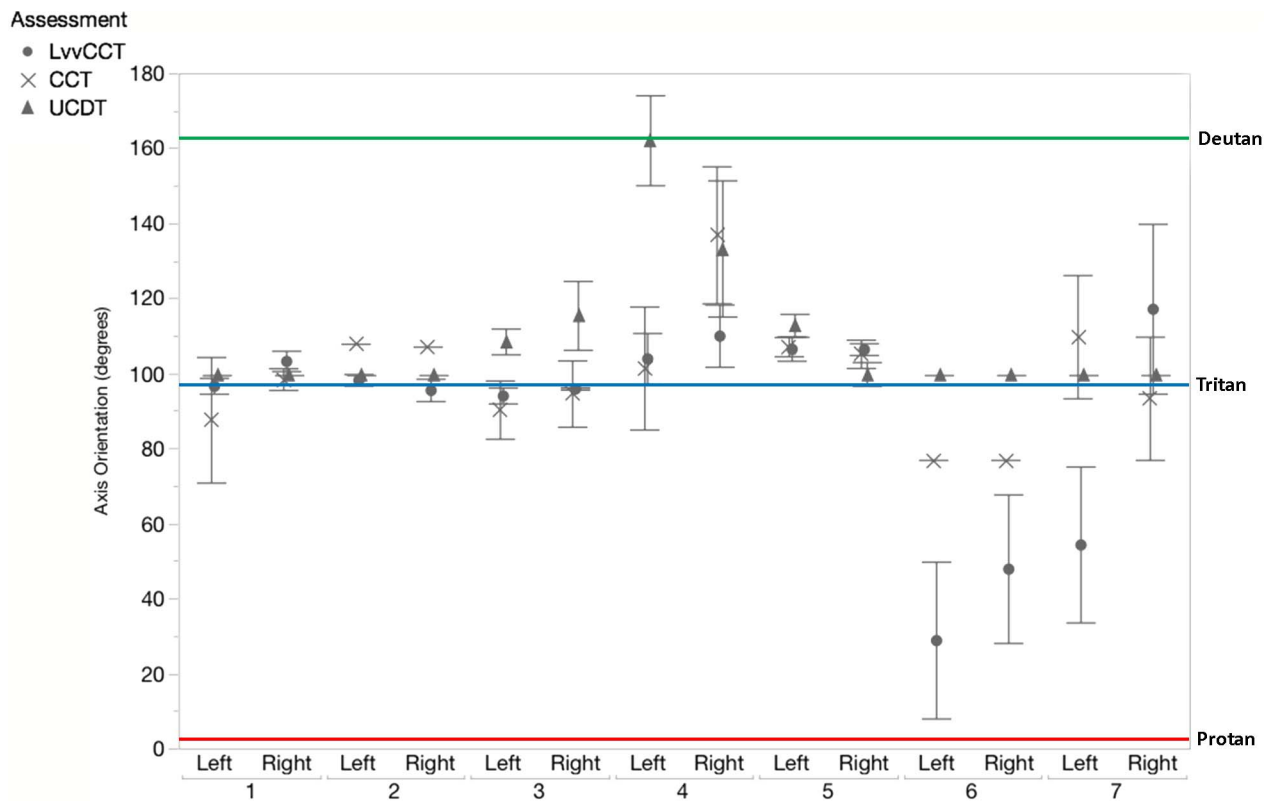


FIGURE 6. Color discrimination Ellipse axis orientation. Shown are the mean (symbols) and one standard error (vertical bars) of the axes of the Ellipse for the lvvcCT, CCT, and UCDT, for each eye of each of the seven tested subjects. The corresponding deutan (green), tritan (blue), and protan (red) confusion axes are also shown.

notable exception to this being the performance of the right eye in subject 4.

Figure 6 shows the mean and standard error of the axes of the best-fit color discrimination Ellipse for each test. The protan, deutan, and tritan axes are also highlighted. As shown, the axes of the majority of the Ellipse assessments fall closest to the tritan axis, in keeping with these subjects having poor color discrimination in the tritan axis.

## DISCUSSION

In this study, we investigated in detail how cone dysfunction affects color vision in a cohort of seven young adults with RPE65-associated LCA. We have identified a severe loss of tritan color discrimination. The lvvCCT Trivector assessment identified significantly worse color discrimination in the tritan axis compared with the protan and deutan axes (Fig. 2). This was further supported by poorer discrimination in the tritan axis, for the majority of patients, as compared with the protan and deutan axes in the CCT and UCDT Trivector assessments, respectively (Figs. 3, 4).

Subjects performed worse overall in the CCT, including four subjects not seeing the stimulus at all. This may be due to their low level of visual acuity preventing them from being able to discern the 1° gap in the C-stimulus. Furthermore, we observed that with the UCDT Trivector assessment, three of seven subjects were also unable to see the stimulus across the three tested axes. All three computerized color vision assessments require subjects to accomplish a visual search to compare the stimulus and the background. We suggest that subjects find the lvvCCT easier than the other two tests, as the stimulus comprises of large (4°) uniform discs, which may be easier to search across. This may explain why the CCT and UCDT are less sensitive in identifying a difference in performance in the tritan, deutan, and protan axes. Interestingly, subject 4, who had the worst level of visual acuity performed variably with the CCT and UCDT. However, when assessed with the lvvCCT, performed more consistently and in keeping with the rest of the cohort.

The Trivector findings, identifying severe loss of tritan color discrimination, are further supported by the axes of the respective Ellipse assessments for the lvvCCT, CCT, and UCDT (Fig. 6).

As tritan color discrimination correlates to S-cone function, we suggest that S-cone function is lost earlier than L- and M-cone function in RPE65-LCA. There are several, not necessarily mutually exclusive, hypotheses that may account for this observation. Firstly, the 'scarcity hypothesis' suggests that if a fixed number of cones are lost, the effect will be greatest on S-cones due to their paucity and hence the overrepresentation of the S-cone signal.<sup>32,33</sup> Secondly, it has been suggested that the S-cone pathway is more vulnerable than that of the L- and M-cones.<sup>34</sup> Finally, it has also been suggested, in mouse models, that L- and M-cones are only partially reliant on the RPE for visual pigment recycling,<sup>35</sup> whereas S-cone reliance on RPE-derived visual pigment has not been explored. It is therefore possible that S-cones may be more reliant on RPE derived visual pigment than L- and M-cones, and hence affected earlier and more severely in the progressive cone dysfunction seen in RPE65-LCA. Further support to our findings in this study can be found from studies in dog and mouse models of RPE65-LCA, where S-cone loss is seen prior to L- and M-cone loss.<sup>36,37</sup>

This study demonstrates the importance of using the most appropriate assessment of color vision. In this cohort of patients only three subjects were able to read any plates using the AO-HRR, a test more often used in clinical care. In comparison, through using the computerized color vision

assessments we were able to quantify color discrimination in all but one subject (Fig. 5) using the Ellipse version of the assessments and identify severe loss of tritan color discrimination as described above. As the lvvCCT shows less variability for those with poorer vision, smaller areas on testing with the ellipse and clearer identification of residual protan and deutan color discrimination, we suggest the lvvCCT to be a more suitable color vision assessment, as compared with the CCT and UCDT, in this cohort of RPE65-LCA adults.

This study demonstrates that color vision can be quantified in most RPE65-LCA subjects. Through using appropriate assessments of color vision, we have identified that these subjects have a severe loss of tritan color discrimination, prior to loss of protan or deutan discrimination. This suggests that S-cone function is lost earlier in the natural history of RPE65-LCA compared with L- and M-cones. Gene therapy for RPE65-LCA has been shown to be safe with varying levels of efficacy and durability noted in both phase I/II and III studies.<sup>6-10,38</sup> Subsequently, multiple new clinical trials are currently underway to investigate potential benefits of gene therapy. Therefore, in-depth assessments of visual function are becoming more critical. Furthermore, knowledge and sensitive assessments of color discrimination are valuable tools in the measurement of the impact of intervention on cone function, both to accurately describe change and to inform patient experience.

## Acknowledgments

The authors thank Melissa Kasilian who assisted with the figures. Supported by grants from the National Institute for Health Research Biomedical Research Centre at Moorfields Eye Hospital NHS Foundation Trust and UCL Institute of Ophthalmology (London, UK), Medical Research Council, Fight for Sight (London, UK), Moorfields Eye Hospital Special Trustees (London, UK), Moorfields Eye Charity (London, UK), Retinitis Pigmentosa Fighting Blindness (Buckingham, UK), and the Foundation Fighting Blindness (Owings, Mills, MD, USA).

Disclosure: N. Kumaran, None; C. Ripamonti, None; A. Kalitzeos, None; G.S. Rubin, MeiraGTx (C); J.W.B. Bainbridge, MeiraGTx (C); M. Michaelides, MeiraGTx (C)

## References

1. Koenekoop RK. An overview of Leber congenital amaurosis: a model to understand human retinal development. *Surv Ophthalmol.* 2004;49:379-398.
2. Stone EM. Leber congenital amaurosis - a model for efficient genetic testing of heterogeneous disorders: LXIV Edward Jackson Memorial Lecture. *Am J Ophthalmol.* 2007;144:791-811.
3. Kumaran N, Moore AT, Weleber RG, Michaelides M. Leber congenital amaurosis/early-onset severe retinal dystrophy: clinical features, molecular genetics and therapeutic interventions. *Br J Ophthalmol.* 2017;101:1147-1154.
4. Acland GM, Aguirre GD, Ray J, et al. Gene therapy restores vision in a canine model of childhood blindness. *Nat Genet.* 2001;28:92-95.
5. Pang JJ, Chang B, Kumar A, et al. Gene therapy restores vision-dependent behavior as well as retinal structure and function in a mouse model of RPE65 Leber congenital amaurosis. *Mol Ther.* 2006;13:565-572.
6. Testa F, Maguire AM, Rossi S, et al. Three-year follow-up after unilateral subretinal delivery of adeno-associated virus in patients with Leber congenital amaurosis type 2. *Ophthalmology.* 2013;120:1283-1291.
7. Weleber RG, Pennesi ME, Wilson DJ, et al. Results at 2 years after gene therapy for RPE65-deficient leber congenital



- amaurosis and severe early-childhood-onset retinal dystrophy. *Ophthalmology*. 2016;123:1606-1620.
8. Jacobson SG, Cideciyan AV, Roman AJ, et al. Improvement and decline in vision with gene therapy in childhood blindness. *N Engl J Med*. 2015;372:1920-1926.
  9. Bainbridge JW, Mehat MS, Sundaram V, et al. Long-term effect of gene therapy on Leber's congenital amaurosis. *N Engl J Med*. 2015;372:1887-1897.
  10. Russell S, Bennett J, Wellman JA, et al. Efficacy and safety of voretigene neparvovec (AAV2-hRPE65v2) in patients with RPE65-mediated inherited retinal dystrophy: a randomised, controlled, open-label, phase 3 trial. *Lancet*. 2017;390:849-860.
  11. Ripamonti C, Henning GB, Ali RR, et al. Nature of the visual loss in observers with Leber's congenital amaurosis caused by specific mutations in RPE65. *Invest Ophthalmol Vis Sci*. 2014;55:6817-6828.
  12. Ripamonti C, Henning GB, Robbie SJ, et al. Spectral sensitivity measurements reveal partial success in restoring missing rod function with gene therapy. *J Vis*. 2015;15(15):20.
  13. Jacobson SG, Aleman TS, Cideciyan AV, et al. Human cone photoreceptor dependence on RPE65 isomerase. *Proc Natl Acad Sci U S A*. 2007;104:15123-15128.
  14. Lorenz B, Poliakov E, Schambeck M, Friedburg C, Preising MN, Redmond TM. A comprehensive clinical and biochemical functional study of a novel RPE65 hypomorphic mutation. *Invest Ophthalmol Vis Sci*. 2008;49:5235-5242.
  15. Paunescu K, Wabblers B, Preising MN, Lorenz B. Longitudinal and cross-sectional study of patients with early-onset severe retinal dystrophy associated with RPE65 mutations. *Graefes Arch Clin Exp Ophthalmol*. 2005;43:417-426.
  16. Curcio CA, Allen KA, Sloan KR, et al. Distribution and morphology of human cone photoreceptors stained with anti-blue opsin. *J Comp Neurol*. 1991;312:610-624.
  17. Hofer H, Carroll J, Neitz J, Neitz M, Williams DR. Organization of the human trichromatic cone mosaic. *J Neurosci*. 2005;25:9669-9679.
  18. Carroll J, Neitz J, Neitz M. Estimates of L:M cone ratio from ERG flicker photometry and genetics. *J Vis*. 2002;2(8):531-542.
  19. Stilling J. *Die Prüfung des Farbensinnes beim Eisenbahn- und Marine-personal*. Cassel: Theodor Fischer; 1877.
  20. Barbur JL. 'Double-blindsight' revealed through the processing of color and luminance contrast defined motion signals. *Prog Brain Res*. 2004;144:243-259.
  21. Regan BC, Reffin JP, Mollon JD. Luminance noise and the rapid determination of discrimination ellipses in colour deficiency. *Vision Res*. 1994;34:1279-1299.
  22. Simunovic MP, Votruba M, Regan BC, Mollon JD. Colour discrimination ellipses in patients with dominant optic atrophy. *Vision Res*. 1998;38:3413-3419.
  23. Ripamonti C, Kalwarowsky S, Nardini M. A Universal Colour Discrimination Test suitable for observers with low vision. *Invest Ophthalmol Vis Sci*. 2014;55:3536.
  24. Chibret JBPL. Contribution a l'etude du sens chromatique au moyen du chromatophotometre. *Revue General d'Ophthalmologie*. 1887;49-59.
  25. MacAdam DL. Visual sensitivities to color differences in daylight. *J Opt Soc Am A Opt Image Vis Sci*. 1942;32:247-274.
  26. Ventura DF, Gualtieri M, Oliveira AG, et al. Male prevalence of acquired color vision defects in asymptomatic carriers of Leber's hereditary optic neuropathy. *Invest Ophthalmol Vis Sci*. 2007;48:236-237.
  27. Ventura DF, Simoes AL, Tomaz S, et al. Colour vision and contrast sensitivity losses of mercury intoxicated industry workers in Brazil. *Environ Toxicol Pharmacol*. 2005;19:523-529.
  28. Costa MF, Oliveira AG, Feitosa-Santana C, Zatz M, Ventura DF. Red-green color vision impairment in Duchenne muscular dystrophy. *Am J Hum Genet*. 2007;80:1064-1075.
  29. Kaernbach C. Simple adaptive testing with the weighted up-down method. *Percept Psychophys*. 1991;49:227-229.
  30. Fitzgibbon A, Pilu M, Fisher R. Direct least-square fitting of ellipses. In: *International Conference on Pattern Recognition*. Vienna, Austria: Proceedings of the 13th International Conference; 1996:253-257.
  31. Paramei GV. Color discrimination across four life decades assessed by the Cambridge Colour Test. *J Opt Soc Am A Opt Image Sci Vis*. 2012;29:A290-A297.
  32. Mollon JD. A taxonomy of tritanopias. *Doc Ophthalmol Proc Ser*. 1982;33:87-101.
  33. Simunovic MP. Acquired color vision deficiency. *Surv Ophthalmol*. 2016;61:132-155.
  34. Greenstein VC, Hood DC, Ritch R, Steinberger D, Carr RE. S (blue) cone pathway vulnerability in retinitis pigmentosa, diabetes and glaucoma. *Invest Ophthalmol Vis Sci*. 1989;30:1732-1737.
  35. Kolesnikov AV, Tang PH, Parker RO, Crouch RK, Kefalov VJ. The mammalian cone visual cycle promotes rapid M/L-cone pigment regeneration independently of the interphotoreceptor retinoid-binding protein. *J Neurosci*. 2011;31:7900-7909.
  36. Mowat FM, Breuwer AR, Bartoe JT, et al. RPE65 gene therapy slows cone loss in Rpe65-deficient dogs. *Gene Ther*. 2013;20:545-555.
  37. Zhang T, Zhang N, Baehr W, Fu Y. Cone opsin determines the time course of cone photoreceptor degeneration in Leber congenital amaurosis. *Proc Natl Acad Sci U S A*. 2011;108:8879-8884.
  38. Bainbridge JW, Smith AJ, Barker SS, et al. Effect of gene therapy on visual function in Leber's congenital amaurosis. *N Engl J Med*. 2008;358:2231-2239.